PROF. DAVID J KELLY (Orcid ID : 0000-0002-0770-6845)

Article type : Research Article

The flavodoxin FldA activates the class 1a ribonucleotide reductase of *Campylobacter jejuni*

Running title: FldA and FqrB activate RNR in *C. jejuni*

Abdulmajeed Alqurashi[1], Laura Alfs[2], Jordan Swann[2], Julea Butt[2] and David J. Kelly[1]*

[1] Department of Molecular Biology and Biotechnology, The University of Sheffield, Firth Court, Western Bank, Sheffield S10 2TN, UK

[2] School of Chemistry, University of East Anglia, Norwich, NR4 7TJ, UK

* Corresponding author: David J. Kelly; e-mail d.kelly@sheffield.ac.uk

Abstract

Campylobacter jejuni is a microaerophilic zoonotic pathogen with an atypical respiratory Complex I that oxidises a flavodoxin (FldA) instead of NADH. FldA is essential for viability and is reduced via pyruvate and 2-oxoglutarate oxidoreductases (POR/OOR). Here, we show that FldA can also be reduced by FqrB (Cj0559), an NADPH:flavodoxin reductase. An *fqrB* deletion mutant was viable but displayed a significant growth defect. FqrB is related to flavoprotein reductases from Gram-positive bacteria that can reduce NrdI, a specialised flavodoxin that is needed for tyrosyl radical formation in NrdF, the beta subunit of class 1b-type (Mn) ribonucleotide reductase (RNR). However, *C. jejuni* possesses a single class 1a-type (Fe) RNR (NrdAB) that would be expected to be ferredoxin dependent. We show that CjFldA is an unusually high potential flavodoxin unrelated to NrdI, yet growth of the *fqrB* mutant, but not the wild-type or a complemented strain, was stimulated by low deoxyribonucleoside (dRNS) concentrations, suggesting FldA links FqrB and RNR activity. Using purified proteins, we confirmed the NrdB tyrosyl radical could be regenerated in an NADPH, FqrB and FldA dependent manner, as evidenced by both optical and electron paramagnetic (EPR) spectroscopy. Thus, FldA activates ribonucleotide reductase in *C. jejuni*, partly explaining its essentiality.

Key words: Flavin, FqrB, Cj0559, flavodoxin reductase, tyrosyl radical

1. Introduction

Campylobacteriosis is the commonest food-borne bacterial zoonosis worldwide, resulting in a huge public health and economic burden, with *Campylobacter jejuni*, as the major causative agent. Under-cooked chicken is the main source of human campylobacteriosis in many countries; 60-80% of cases may be attributable to poulty reservoirs (Sheppard et al., 2009). However, Campylobacters are also found in other farm animals and the environment (e.g. water sources) with both host/source-specific and generalist strains capable of rapid transition between the different physical, nutritional and immunological niches of each host or environment. In humans, *C. jejuni* is an intestinal mucosal pathogen that causes an acute bloody diarrhoea, severe abdominal cramping and fever, with ~0.1% of infections leading to transient paralysis (and occasional deaths) due to inflammatory neuropathies (e.g. Guillain-Barré syndrome). In addition, antimicrobial resistance is a major problem, with an increasing prevalence of fluoroquinolone resistance in particular (Haldenby et al., 2020) and *C. jejuni* has been designated a WHO priority organism for developing novel antimicrobial agents. New insights into *C. jejuni* biology are needed if control measures are to be put in place that more effectively reduce chicken colonisation and/or food-chain contamination.

Campylobacter jejuni is a microaerophile, adapted for growth at low oxygen niches in the host, with most strains unable to grow at atmospheric oxygen levels. Compared to conventional aerobes, *C. jejuni* is unique in utilizing oxidant-labile enzymes in central metabolic pathways, which are critical for growth (Kendall et al., 2014). In particular, it employs pyruvate and 2-oxoglutarate: acceptor oxidoreductases (POR and OOR), rather than oxygen-stable NAD-linked 2-oxoacid dehydrogenases, to transfer substrate-derived electrons to the respiratory chain (Weerakoon and Olson, 2008; Taylor and Kelly, 2019). These enzymes contain Fe-S clusters vulnerable to oxidative damage; we have previously shown that exposure of *C. jejuni* cells to prolonged aeration causes their inactivation *in vivo*, which may be a major contributor to the microaerophilic phenotype (Kendall et al., 2014). Conversely, we could not demonstrate consistent growth under strictly anaerobic conditions, even in the presence of alternative electron acceptors that do allow growth under oxygen-limiting conditions (Sellars et al. 2002). This seems to be due to the presence of a single class 1a-type ribonucleotide reductase (RNR) that would require catalytic amounts of oxygen to sustain DNA synthesis.

The electron acceptor for OOR has been shown to be the flavodoxin FldA (Cj1382; CjFldA), which has a flavin mononucleotide (FMN) cofactor. FldA is the sole flavodoxin encoded in the genome of *C. jejuni* NCTC 11168 (Parkhill et al,. 2000; Weerakoon and Olson, 2008). Reduced FldA is thought to be re-oxidised by donation of electrons from FMN to the membrane bound Complex I of the respiratory chain. In the canonical Complex I found in well studied “model”

bacteria, the *nuoE* and *nuoF* genes encode an NADH-binding module that delivers electrons to Fe-S centres in the NuoG subunit. However, in *C. jejuni*, these genes are replaced by two novel genes *cj1575c* (*nuoX*) and *cj1574c* (*nuoY*), the function of which are unknown (Smith et al., 2000; Calderon-Gomez et al., 2017). Conceivably, they may form a docking site for reduced FldA to deliver electrons to the Fe-S clusters of NuoG (Weerakoon and Olson, 2008; Taylor and Kelly, 2019) but may also have roles independent of Complex I, as unlike all of the other *nuo* genes in *C. jejuni*, *nuoY* (and probably *nuoX*) cannot be deleted (Weerakoon and Olson, 2008). It has also not been possible to delete the *fldA* gene, suggesting that CjFldA must have essential functions (Weerakoon and Olson, 2008). Apart from allowing acetyl-CoA synthesis via POR, one additional likely vital role is in isoprenoid biosynthesis via the methyl erythritol phosphate (MEP) pathway (Heuston et al., 2012). IspG and IspH are 4Fe-4S enzymes that catalyse the last two steps in the formation of the isoprenoid precursors isopentyl pyrophosphate (IPP) and dimethylallyl pyrophosphate (DMAPP); in other bacteria both reactions require reduced flavodoxin as the electron donor (Rohdich et al., 2003; Puan et al., 2005).

A study in the closely related *Helicobacter pylori* (St Maurice et al. 2007) reported that a flavin adenine dinucleotide (FAD) containing and NADPH oxidizing enzyme named FqrB (HP1164) could also act as a flavodoxin reductase in addition to POR. However, based on *in vitro* studies these authors proposed that the physiological function of FqrB was in the production of NADPH via the reversed reaction, i.e. the transfer of electrons from pyruvate to NADPH via POR, flavodoxin and FrqB. In *H. pylori*, FqrB is seemingly an essential enzyme as attempts to produce an *fqrB* deletion mutant were unsuccessful (St. Maurice et al., 2007). A homologue of FqrB (Cj0559) is also present in *C. jejuni*. Here, we show that CjFldA is an unusually high-potential flavodoxin, making NADP reduction unfavourable. Instead, we demonstrate that FqrB provides an additional route for flavodoxin reduction using NADPH as the ultimate electron donor and that both FqrB and FldA are involved in tyrosine radical formation in, and thus activation of, the *C. jejuni* RNR.

2. Results

2.1. Redox properties of the *C. jejuni* flavodoxin: CjFldA is an unusually high redox potential flavodoxin that can be reduced by both POR and OOR

The *C. jejuni* FldA was overexproduced in *E. coli* as a C-terminally his-tagged protein and purified by nickel-affinity and hydrophobic interaction chromatography (Fig. S1A). The as-purified

(oxidized) protein has a typical flavodoxin absorption spectrum (Fig. 1A; raw data for all figures in Table S1) with maxima at ~380 and ~460 nm that matched those of a previous study reporting the purification of this protein (Weerakoon and Olson, 2008). The semi-reduced protein displays a shift of the 380 nm peak to 360 nm and broad absorbance maxima at ~ 460 nm and ~600 nm that are characteristic of neutral semiquinone (Fig. 1A). The latter was exploited in optically monitored potentiometric titrations (Fig. 1B), to define the flavodoxin reduction potentials at pH 7 of -170 mV vs Standard Hydrogen Electrode (SHE) for the oxidized-semiquinone transition (Q/SQ or E_2) and -190 mV vs SHE for the semiquinone-hydroquinone transition (SQ/HQ or E_1).

Independent assessment of the redox properties of CjFldA was afforded by cyclic voltammetry, a powerful electrochemical method to analyse the current response of a redox species with a linearly cycled potential (Fig. 1C). For these experiments the flavodoxin was deposited onto the surface of a pyrolytic graphite edge electrode coated with the surfactant didodecyldimethylammonium bromide (DDAB) (Rusling, 1998; Seagel et al., 2017). Cyclic voltammetry revealed two redox processes. The lower potential process had a mid-point potential of approx. -250 mV, while the higher potential process had a mid-point potential of approx. -150 mV. Neither process was present in voltammetry of DDAB-coated electrodes that had not been exposed to flavodoxin (Fig. 1C). Thus, we assign the processes observed with the CjFldA sample to FMN either within FldA or that had dissociated from the protein. Direct electrochemistry of bacterial flavodoxins using solid electrodes, has been reported by several groups (Barker, 1988; Heering and Hagen, 1996; Seagel et al., 2017). From those findings there are two points of particular significance for interpretation of the voltammetry of CjFldA. Firstly, peaks for the SQ/HQ transformation are well-defined while those of the Q/SQ transformation are typically absent. Secondly, free FMN typically contributes peaks with a mid-point potential of approx. – 200 mV at pH 7. The voltammetry of CjFldA is consistent with Q/SQ *and* SQ/HQ mid-point potentials above -300 mV vs SHE. This conclusion is in agreement with the results from potentiometric titration. Based on voltammetry of CjFldA measured at several independently prepared electrodes and inspection of the relative peak heights and widths for the two processes, it is likely that the higher potential peaks describe the contribution of free FMN. However, we cannot rule out a contribution from the Q/SQ process at these potentials as noted in the voltammetry of *Azotobacter vinelandii* flavodoxin II studied at similarly DDAB-coated graphite electrodes (Seagel et al., 2017).

The E_1 and E_2 redox potential values determined from optical potentiometry (Fig. 1B) are remarkably similar and the E_1 value is far more electropositive than many flavodoxins (Table 1), despite the FMN isoalloxazine binding regions of CjFldA (the W-loop and Y-loop regions; Sancho,

2006) containing several D and E residues that might be expected to destabilize the anionic hydroquinone and shift the E_1 potential to more negative values (Table 1). This is further considered in the Discussion.

The ability of FldA to act as electron acceptor for the POR and OOR enzymes was tested by adding cell-free extract plus CoA to the protein under anaerobic conditions and initiating the reaction by addition of either pyruvate or 2-oxoglutarate. A rapid reduction in the FMN absorbance in the 460 nm region was observed with either substrate (Fig 1D). While FldA has previously been identified as the electron acceptor for OOR (Weerakoon and Olson, 2008) these results show that POR also reduces FldA.

2.2. Cj0559 (FqrB) is an NADPH: flavodoxin reductase related to those in Gram-positive bacteria

Cj0559 in *C. jejuni* is 46.3% identical with FqrB (HP1164) in *H. pylori* strain 26695 and these proteins are members of the large family of FAD containing pyridine nucleotide disulfide oxidoreductases (PNDORs), which include glutathione, CoA disulfide and mercuric reductases, although they do not contain a catalytic disulfide found in some other members of the family such as the thioredoxin reductases. The study of St. Maurice et al. (2007) highlighted the conservation of FqrB-like proteins in the Campylobacterota but similarities with PNDOR enzymes outside this group are less clear. Fig 2A shows a phylogenetic analysis of *C. jejuni* Cj0559 and a range of PNDOR homologues identified by BLAST analysis. It is apparent that the Episilonproteobacterial enzymes, including Cj0559, cluster with a specific group of reductases from Gram-positive bacteria found in *Bacillus subtilis* (YpdA) and *B. cereus/B.anthracis* (FNR3) but are distinct from thioredoxin reductases and CoA disulphide reductases. YpdA is a putative bacillithiol disulphide reductase (Gaballa et al., 2010; Mikheyeva et al., 2019) and FNR3 enzymes have been characterized as flavodoxin reductases; *B. cereus* FNR3 can reduce NrdI, a specific flavodoxin required for formation of the tyrosyl radical in the Mn-containing class 1b RNR's in many Gram-positive bacteria (Lofstad et al., 2016). The FNR1 and FNR2 enzymes also reduce NrdI, with FNR2 being most efficient (Lofstad et al., 2016), but these are more distantly related to FqrB (Fig. 2A).

We tested the ability of the purified C-terminally his-tagged recombinant Cj0559 to act as an NAD(P)H-dependent reductase for the flavodoxin FldA. *C. jejuni* Cj0559 was heterologously overproduced and purified (Fig. S1B) as a yellow-coloured protein with an absorption spectrum typical of a flavoprotein with maxima at ~375 nm and ~460 nm (Fig. 2B). In aerobic buffer at pH

7.5 it exhibited a low rate of NADPH oxidase activity (0.79 ± 0.07 μmol min^{-1} mg $protein^{-1}$, n = 3 determinations), but activity with NADH was over 10-fold lower (0.06 ± 0.01 μmol min^{-1} mg $protein^{-1}$, n = 3). When incubated under strictly anaerobic conditions with a molar excess of FldA, FqrB readily catalyzed the reduction of FldA with NADPH (Fig. 2C and inset) but not with NADH (Fig. 2D and inset). Using an estimated extinction coefficient for flavodoxin FMN of 12 mM^{-1} cm^{-1} at 460 nm (Mayhew and Tollin, 1992) we determined a rate of 14.5 ± 0.2 μmol FMN reduced min^{-1} mg FqrB $protein^{-1}$ with NADPH as reductant (n = 3). These data show that *C. jejuni* FqrB is an efficient FldA reductase specific for NADPH.

2.3. The growth defect of an *fqrB* mutant is partially responsive to deoxyribonucleosides

Given the phylogenetic relationship noted above between FqrB and some NrdI reducing PNDOR enzymes in Gram-positive bacteria, and the identification of FqrB as a redox partner for FldA, we sought *in vivo* evidence that FqrB might be involved in ribonucleotide reduction. Although *hp1164* (*fqrB*) was reported to be essential in *H. pylori*, we were able to construct a deletion mutant in the *cj0559* gene by replacing most of the coding region with a non-polar kanamycin resistance cassette via allelic exchange mutagenesis (see Experimental Procedures). The mutant was also complemented with a wild-type gene copy inserted at the *cj0046* pseudogene locus, driven by the *metK* promoter. The mutant formed small colonies on plates and in liquid culture on complex media it exhibited a significant growth defect compared to the wild-type and complemented strain (Fig. 3A). When grown with a mixture of all four deoxyribonucleosides (dRNS) at 0.1 mM each (final concentration), the growth of the wild-type and complemented strain were not significantly different from that of the controls, whereas the mutant showed an increased growth rate. Interestingly, in the presence of a higher concentration (1 mM each) of dRNS, the growth rate and final cell density of the wild-type and complemented strain were severely inhibited, an effect probably due to an imbalance in the intracellular concentrations of DNA precursors (Torrents 2014). However the growth of the *fqrB* mutant was much less affected (Fig. 3A). The mutant was also significantly less sensitive to the toxic nucleotide analogues 6-thioguanine and 6-mercaptopurine compared to the wild-type and complemented strains (Fig. 3B). Taken together, these results suggest that the lack of FqrB in the mutant affects dRNS uptake and metabolism; a slower conversion of ribonucleotides to deoxyribonucleotides via ribonucleotide reductase might explain the partial growth stimulation by exogenous dRNS. We further investigated the link between FqrB and RNR by *in vitro* studies with the beta subunit of the RNR.

2.4. Characterisation of NrdB, the RNR beta subunit of *C. jejuni*

Campylobacter jejuni NCTC 11168 encodes a single heterodimeric RNR (Parkhill et al., 2000). The alpha subunit (NrdA; Cj0024) is predicted to catalyse ribonucleotide reduction using a cysteine radical, generated by long-range transfer from a tyrosine radical formed in the beta subunit (Cj0231). In class Ia RNRs, the tyrosine radical in NrdB is generated by oxygen and electrons from two reduced iron centres in a μ-oxo-bridged configuration, while in class 1b enzymes which have oxygen unreactive manganese ions instead of iron, superoxide generated by a reduced flavodoxin (NrdI) is used to form the radical in the beta subunit, designated NrdF (Stubbe and Cotruvo, 2011). As noted above, NrdI is itself reduced by a specific reductase of the PNDOR family. The dRNS growth stimulation observed in the *C. jejuni fqrB* mutant (Fig. 3A), could be explained if radical formation in the *C. jejuni* RNR required FldA, with FqrB acting as a physiologically relevant flavodoxin reductase. However, CjFldA is distinct from NrdI proteins and the alpha and beta subunits of *C. jejuni* RNR and other Campylobacterota are related to other class 1a NrdA and NrdB proteins from Gram-negative bacteria (although it should be noted that Cj0231 is currently annotated as NrdF). The *C. jejuni* NrdA subunit also has a typical N-terminal ATP-cone domain that is characteristic of a class 1a enzyme (Hofer et al., 2012). Therefore, we wished to test if radical formation in *C. jejuni* NrdB required flavodoxin, by producing purified radical free NrdB and reconstituting with FldA, FqrB and NADPH to determine if the radical could be regenerated *in vitro*.

NrdB was overproduced in *E. coli* BL21 (DE3) as a C-terminally his-tagged protein and purified by nickel affinity chromatography. Two bands were consistently seen on SDS-PAGE gels (Fig. S1C), an upper band corresponding to the expected size of NrdB-6His (~40.5 kDa) and a lower band of ~35 kDa. Both bands were trypsin digested and subjected to HPLC-LC/MS. The same NrdB peptides were detected in both bands (Fig. S2 and Table S2), including from both the N-terminal and C-terminal regions of NrdB, showing that the lower band is not a contaminant or N-terminally truncated version of the upper band. It most likely arises due to an unidentified post-translational modification, which causes faster mobility on SDS-PAGE. The metal content of independently purified batches of the protein was determined by ICP-MS after growth in either unsupplemented, iron- or manganese supplemented media (Fig. 4A). In each case, the molar ratio of Fe/protein (1.0, 1.4 and 0.85 respectively) was significantly higher than the Mn/protein ratio (0.14, 0.05 and 0.25 respectively). Overall, the data confirm that the *C. jejuni* RNR is indeed an Fe enzyme of the class 1a type and that the database annotation of Cj0231 as NrdF is incorrect. Although the expected ratio of Fe/monomer is 2, a suboptimal stoichiometry is commonly found in heterologously expressed RNRs (Roca et al., 2008). The optical absorption spectrum of the protein shows a typical sharp feature at 410-411 nm diagnostic of the presence

of a stable tyrosyl radical as well as weaker charge transfer bands centred around 325 nm and 370 nm arising from the μ-oxo-bridged diferric centre. We found that treatment of the protein with 1 mM of the radical scavenger hydroxylamine (HA) for 30 min efficiently removed the tyrosyl radical, as evidenced by the disappearance of the 411 nm band (Fig. 4B). Although the optical spectrum of the HA treated protein also appeared to lack the 370 nm absorbance associated with the di-ferric centre, comparison of the electron paramagnetic resonance (EPR) spectra of the as-purifed and HA-treated protein showed an equivalent feature at g = 4.27 attributable to residual magnetically isolated ferric iron (Fig. 4C). Calculation of the difference spectrum of HA treated versus untreated protein (Fig 4B) and applying a literature value for the extinction coefficient of 3.25 mM cm^{-1} for the radical (Petersson et al., 1980) resulted in an estimation of the radical yield in the purified protein of 0.7 per monomer, comparable with data for other enzymes (Roca et al., 2008). In contrast to hydroxylamine, treatment with the commonly used radical scavenger hydroxyurea (HU) did not result in quenching, even in the presence of the metal chelator EDTA (Fig. 4D).

2.5. Tyrosyl radical regeneration in NrdB can be catalyzed by FldA, FqrB and NADPH

The ability to produce a radical free NrdB preparation allowed us to investigate the requirements for radical formation in this protein. Incubation of HA-treated and dialysed NrdB with an equimolar concentration of the flavodoxin FldA (50 μM) plus a catalytic amount of FqrB (5 μM) and excess NADPH resulted in the build up of the characteristic tyrosyl radical absorbance at 411 nm (Fig. 5A). A series of control incubations lacking any single component of this mixture resulted in no increase in absorbance at 411 nm (Fig 5B), showing that radical formation was dependent on reduced flavodoxin formed through the NADPH dependent reductase activity of FqrB. In order to further confirm that the tyrosyl radical had indeed been re-generated in the reconstituted system with characteristics similar to the native NrdB, we compared the EPR spectrum of a sample of as-purified NrdB with HA-treated NrdB and that obtained after reconstitution with NADPH, FqrB and FldA. The optical spectra of the same samples used for EPR are shown in Fig. 5C, which again confirm the presence of the 411 nm band after reconstitution, and the corresponding 10 K EPR spectra are shown in Fig. 5D. Essentially identical EPR spectra were recorded from both the as-purified protein and after reconstitution with NADPH, FqrB and FldA (Fig. 5D). The spectra also show that HA treatment effectively removed the radical from NrdB, with only very weak EPR signals remaining. The centre of the free radical EPR signals is at ~ g = 2.0052 and the lineshape is typical of that of Fe_2-tyrosyl radical containing class 1a RNRs (Hoganson and Babcock, 1992; Sahlin et al. 1987).

2.6. Is superoxide involved in FldA catalysed tyrosyl radical formation ?

The di-ferrous centre in class Ia RNRs is readily oxygen reactive and the electron input required for re-reduction has been proposed to be supplied in some bacteria by a small ferredoxin, YfaE (Wu et al., 2007). *yfaE* is sometimes genetically linked to the *nrdAB* genes but is not present in Campylobacterota including *C. jejuni*. Given the *C. jejuni* RNR is a class 1a enzyme it seems most likely that the role of FldA identified above is as a simple electron donor to NrdB in place of YfaE. However, in class 1b RNRs that use oxygen unreactive Mn as cofactor, the NrdI flavodoxin generates superoxide which acts as the oxidant to form the tyrosyl radical (Berggren et al., 2014). The possible involvement of superoxide in the regeneration of the tyrosyl radical in the *C. jejuni* NrdB by reduced FldA was investigated in two ways. First, we added excess superoxide dismutase to a mixture of FqrB, FldA and HA-treated NrdB before adding NADPH to start the reaction. After prolonged incubation, tyrosyl radical formation was only slightly suppressed compared to incubations lacking SOD (Fig 6A and 6B), but was still readily detectable. The caveat here is that superoxide could be channeled from flavodoxin to NrdB by close interaction, so may not be sensitive to SOD (Bergrren et al., 2014). Secondly, we incubated purifed HA-treated NrdB with the well-known xanthine oxidase/hypoxanthine superoxide generating system, as a way of generating superoxide independently of flavodoxin and FqrB. A time dependent formation of the tyrosyl radical could be observed, as evidenced by the absorbance increase at 411 nm (Fig. 6C). This suggests that at least *in vitro* superoxide can result in tyrosyl radical formation in *C. jejuni* NrdB.

3. Discussion

As the electron acceptor for the citric-acid cycle enzymes POR and OOR, FldA is a central redox shuttle in the physiology of *C. jejuni*, but other roles for this key protein have not been investigated and genetic studies are hampered by its essentiality. In this work, we have identified the *cj0559* encoded FqrB as a FldA reductase and phenotypic analysis of a deletion mutant lacking FqrB has revealed a hitherto unknown link between FldA and deoxyribonucleotide reduction.

FqrB from *C. jejuni* is an NADPH specific flavodoxin reductase that has a phylogenetic relationship to a group of similar enzymes from Gram-positive bacteria, some of which are known to be redox partners for NrdI-like flavodoxins necessary for tyrosyl radical formation in class 1b

RNRs. FqrB was initially identified in *H. pylori* as a quinone and flavodoxin reductase that was suggested to participate in the production of NADPH by operating in the reverse direction to that proposed here, i.e. coupling the reduction of NADP to the oxidation of reduced flavodoxin that had been generated by the action of POR (St Maurice et al., 2007). This seemed to confirm earlier data from the study of Hughes et al. (1998) who detected pyruvate, CoA and FldA dependent NADPH production in *H. pylori* cell-free extracts. The same reaction could also be demonstrated in *C. jejuni* crude extracts (St Maurice et al., 2007). However, the rates of NADPH production in these studies were very low (of the order of a few nmol min^{-1} mg $protein^{-1}$). We can now explain this in view of the relatively high midpoint redox potential of FldA (-180 mV) compared to NADPH (-320 mV), such that it is thermodynamically unfavourable for FldA to reduce NADP. It is therefore unlikely that this mechanism would be relevant *in vivo* and it should be noted that other known enzymes in *C. jejuni* central metabolism operate to reduce NADP directly (e.g. isocitrate dehydrogenase). On the contrary, our data suggest that FqrB catalyses NADPH dependent reduction of FldA, in addition to POR and OOR, and this contributes to the maintenance of a reduced pool of FldA for diverse metabolic reactions requiring this electron carrier (Fig. 7). That NADPH can reduce FldA might also explain previous reports of (albeit low) NADPH dependent respiration in membranes and cell extracts of campylobacters (Lascelles and Calder, 1985; Weerakoon and Olson, 2008).

The phenotype of an *fqrB* deletion mutant implicates FqrB in ribonucleotide reduction. The fact that this mutant was viable, although with a large growth defect, is presumably because POR and OOR are also still able to contribute to FldA reduction. Although POR is essential (Kendall *et al*., 2014), presumably because there is no other way to make acetyl-CoA, an *oorB* mutant has previously been reported (Weerakoon and Olson, 2008). The stimulation of *fqrB* mutant growth by dRNS was significant although not large in magnitude, but this would be consistent with the additional functions that FldA has in electron transport to Complex I and e.g. isoprenoid biosynthesis (Fig. 7) as well as other possible cellular redox processes yet to be identified. It should also be noted that although a potential transport system and phosphoribosyl phosphotransferase for nucleotide salvage has been identified in *C. jejuni* (Yahara et al., 2017), Campylobacterota including *C. jejuni* are not thought to possess a deoxyribonucleoside kinase that would efficiently phosphorylate these precursors (Sandrini et al., 2006; Konrad et al., 2012), which could account for the poor growth response observed. It is also possible that FqrB can reduce other, as yet unidentified, redox partners that are important for optimum growth.

Biochemical evidence for a role of FqrB and FldA in RNR activation was obtained by an *in vitro* reconstitution approach with the relevant purified proteins. The tyrosyl radical in purified NrdB

was remarkably resistant to quenching by hydroxyurea, despite growth being sensitive to this compound and causing filamentation in treated cells consistent with RNR inhibition (Sellars et al., 2002). Hydroxylamine proved an effective radical scavenger however and we were able to show, with appropriate controls, that radical re-formation could be promoted in the presence of NADPH, FqrB and FldA. Importantly, the EPR data show that the characteristics and environment of the radical formed *in vitro* is indistinguishable from that in the as-purifed NrdB protein. The *fqrB* mutant phenotype data taken together with the *in vitro* reconsitution experiments therefore support a physiological role for FqrB and FldA in NrdB tyrosyl radical formation, and thus ribonucleotide reduction, in *C. jejuni*, as illustrated in Fig. 7. Although our data was obtained with strain NCTC 11168, FqrB, FldA and NrdB are present in other strains of *C. jejuni* and, for example, are 97-100% identical in two other commonly studied strains, 81-176 and 81116. The model in Fig. 7 should therefore be generally applicable.

We have characterized FldA in this work as a high redox potential flavodoxin, with the $FldA_{ox}/FldA_{sq}$ and $FldA_{sq}/Fld_{hq}$ couples having E_m values of -170 mV and -190 mV respectively. Before we consider the significance of this in relation to RNR, it is worth noting the implications of these redox properties for understanding the bioenergetics of Complex I in *C. jejuni*, which uses FldA as the electron donor instead of NADH. Aerobic bacteria that use NADH (E_m -320 mV) coupled with ubiquinone (E_m +100 mV) as the electron acceptor for Complex I will have an overall ΔE of ~420 mV to drive proton translocation electrogenically, against an existing Δp of ~180 mV. However, only menaquinone-8 (MK-8) and methylmenaquinone-8 (mMK-8) are present in *C. jejuni* membranes (Carlone and Anet, 1983). The E_m for MK-8 is about -75 mV and for mMK-8 it is -124 mV (Junkhe et al., 2009) or as low as -140 mV (Hein et al., 2018). The ΔE for FldA reduction of MK-8 is therefore only ~ 100 mV and for mMK-8 it is ~50 mV; considerably lower than Δp. Unless the *in vivo* redox potentials of the menaquinones and/or the FldA flavin are considerably different from those measured in solution, it remains an open question if electrogenic proton pumping can occur through Complex I in *C. jejuni* (see also Taylor and Kelly, 2019). Interestingly, direct measurements of Δp in intact *C. jejuni* cells using ion-selective electrodes showed that pyruvate produced the lowest Δp compared to electron donors like formate, that do not couple with FldA (van der Stel et al., 2017).

Canonical flavodoxins involved in electron transport usually have a wide separation in their E_1 and E_2 redox potentials, due to a negative electrostatic environment around the isoalloxazine ring of the FMN, causing destabilization of the hq form and shifting the E_1 potential much more negative than free FMN. For example, *Desulfovibrio vulgaris, Synechocystis* and *Azotobacter*

vinelandii all have E_1 values of < -400 mV (Table 1). This is also reflected in the pI values of such flavodoxins, which are usually acidic. NrdI proteins, however, have a bi-modal distribution with both low pI (mainly Firmicutes) and high pI (*E. coli* and most other proteobacteria) types (Johansson et al., 2010). Both types tend to have a more neutral (or charge compensated) environment in the loops surrounding the bound FMN, resulting in higher and often more similar E_1 and E_2 redox potentials than canonical flavodoxins (Table 1), but the picture is quite complex and other residues are also important.

The *C. jejuni* FldA is a long-chain flavodoxin with a predicted pI of 3.9 and it possesses conserved anionic residues in the W- and Y-loop regions involved in FMN binding (Table 1) that might be expected to result in a much lower E_1 redox potential than the -190 mV determined here. A crystal structure will be needed to rationalize the reasons for this disparity. Nevertheless, the similarity in the smaller separation in the E_1 and E_2 potentials of FldA and most NrdI proteins is intriguing. In class 1a RNRs a small ferredoxin, exemplified by YfaE in *E. coli* (Wu et al., 2007) has been implicated in supplying electrons to reduce the di-ferric centre in NrdB to allow oxygen to react with the di-ferrous state, necessary to form the tyrosyl radical. No homologue of YfaE exists in *C. jejuni* and indeed only 29% of 181 NrdAB containing genomes were found to encode a *yfaE*-like gene linked to *nrdAB* (Wu et al., 2007), implying that in most bacteria, other redox proteins satisfy this requirement. Our data suggests that *C. jejuni* uses the flavodoxin FldA instead of a ferredoxin as the electron donor to NrdB. YfaE is a 2Fe-2S ferredoxin that directly supplies electrons, one at a time, to reduce the NrdB diferric centre (Wu et al., 2007). FldA, with E_1 and E_2 separated by only 20 mV could act in a similar manner. Nevertheless, *in vitro* generated superoxide also formed the radical in NrdB, as found with the NrdI flavodoxins interacting with the class 1b NrdF (Berggren et al., 2014). However, the physiological significance of this is difficult to judge, given that the NrdB/class 1a type of Fe-containing RNR should be fully capable of generating the Tyr radical from the oxidation of ferrous to ferric iron at the di-iron centre mediated by molecular oxygen alone. It would clearly be informative to examine the relative reactivity of the *C. jejuni* NrdB di-iron centre with superoxide versus oxygen in more detail.

In conclusion, our results explain why the sole flavodoxin of *C. jejuni* is essential and provide experimental evidence for at least one key role unrelated to respiratory electron transport. Recent work on the *H. pylori* FldA has resulted in the development of inhibitors that are novel drug candidates for therapeutic use (Salillas and Sancho, 2020), highlighting how the unique biochemistry of essential proteins like flavodoxin in pathogenic Campylobacterota can be exploited.

4. Experimental Procedures.

4.1. Bacterial strains and growth conditions

Campylobacter jejuni NCTC 11168 was routinely grown at 42 °C in microaerobic conditions [10% (v/v) O_2, 5% (v/v) CO_2 and 85% (v/v) N_2] in a MACS growth cabinet (Don Whitley Scientific, Shipley, UK). Columbia blood agar plates containing 10 μg ml^{-1} each of amphotericin B and vancomycin were used for routine subculture. For *fqrB* mutant selection kanamycin was additionally used in blood agar plates at 50 μg ml^{-1} and for selection of the complemented mutant, both kanamycin and apramycin (50 μg ml^{-1} each) were included. Cells from plates were inoculated into 25 ml starter cultures in Mueller-Hinton broth supplemented with 20 mM L-serine and 10 μg ml^{-1} each of vancomycin and amphotericin B (MHS media). Starter cultures were incubated on a shaker at 150 rpm in the MACS growth cabinet for 12-16 h followed by inoculation into growth cultures (30-500 ml) to a starting OD_{600} of ~0.1. *Escherichia coli* strains were grown aerobically in LB media at 37 °C. Where required ferrous ammonium sulphate or manganese chloride was added to 100 μM final concentration and carbenicillin used at 50 μg ml^{-1}.

4.2. Construction of an *fqrB* mutant and complemented strain.

Isothermal assembly (ISA) cloning (Gibson et al., 2009) was used to generate a plasmid for transformation into *C. jejuni*, that deletes *cj0559* (*fqrB*) by allelic exchange mutagenesis, replacing most of the coding region with a kanamycin resistance cassette derived from pJMK30 (van Vliet et al., 1998), which carries a constitutive promoter and no terminator. The ISA reaction assembled 4 PCR amplified fragments; HincII digested pGEM3Zf(-) vector, two regions of ~ 500 bp flanking *cj0559*, such that only the first few and last few codons of the gene were retained, and the kanamycin resistance cassette, to be inserted between the two flanking regions. The kanamycin resistance cassette was amplified from pJMK30 using primers Kan_F and Kan_R (Table 2). The left flanking region of the gene was amplified using primers FQRB_ISA_F1F and F1KR (Table 2) and the right flanking region was amplified by FQRB_ISA_F2KF and F2R. The F1F and F2R primers contain 30 bp adapters for the pGEM3Sf(-) vector cut with HincII and the F1KR and F2KF primers contain 30 bp adapters for the kanamycin resistance cassette. PCR amplifications were performed with Phusion polymerase (NEB). The ISA reactions were performed as previously described (Liu and Kelly, 2015) and used to directly transform competent *E. coli* DH5α cells, with selection on LB + kanamycin agar plates. Colonies were screened by PCR with using different combinations of KAN, ISA and standard M13 primers. Correct plasmids,

designated pGEMFQR were confirmed by automated DNA sequencing (Core Genomic Facility, University of Sheffield Medical School, UK). pGEMFQR was electroporated into *C. jejuni* NCTC 11168 and cells plated out on Columbia agar plates, incubated overnight in microaerobic conditions at 42 °C. The growth was then transferred to Columbia blood agar plates plus kanamycin and incubated for 3 days. Correct mutants were identified by colony PCR with ISA and KAN primers. To complement this mutant with the wild-type *fqrB* gene driven by its native promoter, the gene plus ~200 bp upstream sequence was amplified with primers FQRB_COMP_F and FQRB_COMP_R (Table 2) and cloned into the pRRA vector (Cameron and Gaynor, 2014) at MfeI and XbaI sites. This recombines the gene at one of the 16S rRNA loci. This plasmid was electroporated into the *fqrB* mutant and colonies selected on Columbia blood agar plates plus kanamycin and apramycin.

4.3. Overproduction and purification of proteins

The *fqrB*, *fldA* and *nrdB* genes were cloned between the NdeI and XhoI sites of the pET21a vector (Novagen) such that a 6-his tag was attached in-frame to the C-terminus of the cognate proteins. The primers used are shown in Table 2. Each plasmid was transformed into *E. coli* BL21(DE3), grown in 1-5 L batches of LB media (plus carbencillin 50 μg ml^{-1}) at 37 °C to an OD 600 nm of 0.5, then protein production induced by 0.4 mM isopropyl-thiogalactoside (IPTG) for up to 3 h (FldA), 5 h (FqrB) or 6 h (NrdB). Cells were harvested by centrifugation (10,000 x *g*, 10 min, 4 °C), resuspended in binding buffer (20 mM sodium phosphate buffer pH 7.6, 0.5 M NaCl, 20 mM imidazole plus one Protease Inhibitor Mini Tablet [Pierce; Thermo Fisher Ltd, UK] per 20 ml), 10 units ml^{-1} DNAse I added (from bovine pancreas; Sigma Aldrich) and the cells disrupted by French Press (SLM Aminco) followed by centrifugation (15,500 x g, 10 min, 4 °C) to remove debris. The supernatants were filtered (0.45 μm pore size) and pumped onto a 5 ml-HisTrap HP column (GE healthcare, UK) pre-equilibrated with binding buffer, connected to an AKTA Prime Protein Purification System. Proteins were eluted with a linear gradient of elution buffer (20 mM sodium phosphate buffer pH 7.6, 0.5 M NaCl, 0.5 M imidazole). For FldA and FqrB, further purification using hydrophobic interaction chromatography (HIC) was performed using a 5 ml Phenyl sepharose HIC column (GE healthcare, UK), with proteins bound in 50 mM Tris-HCl buffer pH 7.5 + 1.5 M ammonium sulphate and eluted with a linear gradient of 50 mM Tris-HCl buffer pH 7.5. After purification, proteins were buffer exchanged into 50 mM Tris-HCl pH 7.5 using Vivaspin spin columns (Sartorius Stedim) with a molecular weight cut-off of at least 50% smaller than the protein size. Protein purity was assessed by SDS-PAGE.

4.4. Mass spectrometry of NrdB

The two bands seen on SDS-PAGE gels of purified NrdB were cut out, divided into small pieces and de-stained in 500 µl acetonitrile/ammonium bicarbonate buffer (a 1:1 mixture of acetonitrile and 100 mM ammonium bicarbonate, pH 8.0). The supernatant was removed and the gel pieces were washed thrice with the same buffer then dehydrated with 500 µl acetonitrile for 10 minutes. 200 µl of 50 mM Tris(2-carboxyethyl)phosphine (TCEP) in 100 mM ammonium bicarbonate buffer pH 8.0 was added to reduce cysteines, with incubation for 20 minutes at 70 °C. The supernatant was discarded and cysteines acetylated with 200 µl of 50 mM iodoacetamide in ammonium bicarbonate buffer. Gel pieces were then washed and dehydrated as above. For trypsin digestion, gel pieces were incubated in 200 µl of 1 ng µl-1 trypsin (Thermo Fisher Scientific) in ammonium bicarbonate buffer overnight at 37 °C. 100 µl of acetonitrile was added the next day and gel pieces were incubated for 15 minutes at 37 °C. The digested peptides released in the supernatant were collected in a separate tube. 50 µl of 0.5 % v/v formic acid was added to the gel pieces and after 15 minutes 100 µl of acetonitrile was added and incubated for an additional 15 minutes. The supernatant was transferred to the collection tube and the extraction with formic acid and acetonitrile repeated. Finally, the combined supernatant was incubated with 100 µl of acetonitrile for 15 minutes resulting a final volume of 700 µl of digested peptides, which were dried down using a SpeedVac concentrator. To analyse the peptides via HPLC-MS, the pellet was resuspended in 40 µl 0.5 % v/v formic acid. 20 µl of peptide solution was transferred to vials and analysed by the Biological Mass Spectrometry Facility at The University of Sheffield. HPLC was done at 45 °C using a Dionex UltiMate 3000 system (Thermo Fisher Scientific) equipped with an Acclaim™ PepMap™ 100 C18, 20 mm x 75 µm Trap column (3 µm diameter particles, 100 Å pore size) and an EASY-Spray™ C18, 150 mm x 50 µm (2 µm diameter particles, 100 Å pore size) analytical nano-column. Mobile phase A consisted of 0.1 % v/v formic acid in water and mobile phase B consisted of 0.1 % v/v formic acid in 80 % v/v acetonitrile. The gradient was formed at a flow rate of 250 ml min-1 as follows: 0-5 minutes at 4 % B, then two steps of linear increase; first 40 % B for 40 minutes then 90 % B for 50 minutes. An LTQ Orbitrap Elite (Thermo Fisher Scientific) hybrid ion trap-orbitrap mass spectrometer and an EASY-Spray source with an ion transfer capillary at 250 °C and a voltage of 1.8 kV were used for MS analysis. MS survey scans in positive ion mode were acquired in the FT-orbitrap analyzer using a m/z window from 375 to 1600, a resolution of 60,000, and an automatic gain control target setting of 1 x 106. Using collision induced dissociation (CID), the 20 most intense precursor ions were selected for the acquisition of tandem mass spectra in the dual cell linear ion trap at normal scan rate. Charge states 1+ were not included for precursor selection. Normalized collision energy was set to 35 %, activation time to 10 ms, isolation width to 2 m/z, and automatic gain control value was set to 1 x

104. Identification of peptides/proteins was performed by MaxQuant (Cox and Mann, 2008), searching with default parameters.

4.5. ICP-MS

Purifed NrdB samples were added to 1 ml concentrated HNO_3 (65% v/v), left in acid overnight and then analysed at the University of Sheffield ICP-MS facility.

4.6. Optical spectroscopy

Mediated potentiometric titration monitored by electronic absorbance spectroscopy was performed by the method of Dutton et al. (1970) with minor modification. The reductant was sodium dithionite and the oxidant was potassium ferricyanide. The sample contained 50 μM CjFldA in 10 mM potassium phosphate buffer, pH 7.0 with the following mediators each at 10 μM; diaminodurene (E_m +240 mV), phenazine methosulphate (E_m +80 mV), phenazine ethosulphate (E_m +55 mV), juglone (E_m +30 mV), duroquinone (E_m +5 mV), menadione (E_m -70 mV), anthraquinone 2,6-disulphonate (E_m -184 mV), anthraquinone-2-sulphonate (E_m -225 mV). Flavodoxin semiquinone was quantified from the absorbance at 610 nm using an extinction coefficient of 3900 $M^{-1}cm^{-1}$ (Mayhew et al., 1969). The plot of semiquinone concentration versus sample potential was fitted to the equation describing two sequential one-electron transfers to a single site:

$$\text{semiquinone population} = {}^{1}\!/\!_{(1 + \theta_1 + \theta_2^{-1})}$$

where $\theta_i = \exp(39(E - E_i))$, E is the sample potential and E_1 and E_2 are the reduction potentials for addition of the first and second electron respectively. Equivalent experiments without flavodoxin showed there was negligible spectral change from the mediators at 610 nm for potentials where the semiquinone was observed.

4.7. Protein film electrochemistry

Cyclic voltammetry was performed using a three-electrode cell configuration inside a Faraday Cage within a N_2-filled chamber (atmospheric oxygen < 5 ppm). The reference electrode was Ag/AgCl (saturated KCl) and the counter electrode a platinum wire. The working electrode was pyrolytic graphite with the edge plane exposed to sample. Preparation of the working electrode was essentially as described by Seagel et al (2017). Firstly, the surface was polished with 0.3 μm Al_2O_3 as an aqueous slurry, sonicated, rinsed with Milli-Q water and dried with a tissue. Secondly,

5 µL of 10 mM didodecyldimethylammonium bromide (DDAB) in Milli-Q water was placed on the electrode surface, the electrode covered with a beaker and left to dry overnight at ambient temperature. Finally, the DDAB coated working electrode was taken into the N_2-filled chamber and 5 µL of 200 µM flavodoxin (in 50mM phosphate, 150mM NaCl, pH 7.5) deposited on the surface. After 20 min the working electrode was introduced to the electrochemical cell, which contained an aqueous solution of 50 mM potassium phosphate, pH 7. Cyclic voltammetry was performed with a PGSTAT30 potentiostat (Metrohm Autolab) under the control of NOVA 1.11 software. Measured potentials were converted to values versus SHE by addition of 197 mV.

4.8. EPR spectroscopy

All EPR spectra were measured on a Bruker EMX EPR spectrometer (X-band). A Bruker resonator ER 4122 (SP9703) and an Oxford Instruments liquid helium system were used to measure the low-temperature (10 K) EPR spectra. Wilmad SQ EPR tubes (Wilmad Glass, Buena, NJ, USA) with OD = 4.05 mm and ID = 3.1 mm were used. Aliquots (250 µl) of the samples were placed in the EPR tubes, frozen in methanol and kept on dry ice (~195 K). The EPR tubes were then transferred to liquid nitrogen (77 K) and stored there until the measurements on the EPR spectrometer. Instrument settings are given in the relevant figure legends. The spectra were acquired by Dr Dima Svistunenko at the Biomedical EPR Facility, University of Essex, UK.

4.9. Enzyme assays

All spectrophotometric assays were conducted at 37 °C in a Shimadzu UV-2401 spectrophotometer. The ability of pyruvate and 2-oxoglutarate to act as electron donors to FldA via the action of the POR and OOR enzymes was assayed using cell-free extracts (CFE) of *C. jejuni* prepared by sonication under anaerobic conditions as described previously, in the presence an oxygen-scavenging system consisting of glucose oxidase, glucose and catalase (Kendall et al., 2014). CFE was added to nitrogen-sparged 100 mM Tris-HCl buffer pH 8, 2 mM $MgCl_2$, 0.2 mM Coenzyme A, 0.1 mM thiamine pyrophosphate and 50 µM purifed FldA in stoppered anaerobic cuvettes. The reaction was started by injection of anaerobic pyruvate or 2-oxoglutarate to 5 mM final concentration. Reduction of the FMN of FldA was followed at 460 nm. The NAD(P)H oxidase activity of FqrB was assayed at 340 nm (ε = 6.22 mM^{-1} cm^{-1}) in oxygen saturated 50 mM Tris-HCl buffer pH 7.5 after addition of FqrB (1 µM final) and either NADPH or NADH (300 µM final) to start the reaction. The reduction of FldA by FqrB and NAD(P)H was

measured at 460 nm (estimated ε of 12 mM^{-1} cm^{-1}; Mayhew and Tollin, 1992) in 50 mM Tris-HCl buffer pH 7.5, 50 μM FldA, 0.1 μM FqrB and 150 μM either NADH or NADPH to start the reaction.

4.10. Preparation of radical free NrdB and reconstitution with FqrB, FldA and NrdB

Purified NrdB was treated with 1 mM hydroxylamine for 30 min then repeatedly buffer exchanged into 50 mM Tris-HCl pH 7.5 until no hydroxylamine could be detected. Residual hydroxylamine was detected by reaction with 8-hydroxyquinoline to form green indooxime after heating, which absorbs at 710 nm (Lanvers et al., 2002). Reconstitution assays with radical free NrdB were done in 50 mM Tris-HCl buffer pH 7.5 with 50 μM NrdB, 50 μM FldA, 5 μM FqrB and 1 mM NADPH. Where samples were to be monitored by EPR, the buffer was changed to 20 mM Tris-HCl pH 7.7 plus 50 mM L-arginine and 50 mM L-glutamate to enhance NrdB stability.

4.11. Phylogenetic analysis

Protein sequences were obtained from Uniprot. Multiple sequence alignments were made with CLUSTAL Omega and phylogenetic rees were generated and analysed in JALVIEW, using publicly available software at www.expasy.org.

Acknowledgements

We thank Dr Dima Svistunenko (Director, Biomedical EPR Facility, University of Essex, UK) for obtaining the EPR spectra and Prof Nick Le Brun and Dr Justin Bradley (School of Chemistry, University of East Anglia, UK) for help with EPR and sample preparation. Dr Adelina Acosta-Martin performed MS analysis of the NrdB samples. AA was the recipient of a PhD scholarship from the Ministry of Higher Education of the Government of Saudi Arabia.

Author contributions

Conception and design of study; DJK. Acquisition, analysis and interpretation of data; AA, LA, JS, JB, DJK. Writing of the manuscript; DJK, JB, AA.

Data availability statement

The data that supports the findings of this study are available in the supplementary material of this article (Tables S1 and S2).

References

Barker, P.D., Hill, H.A.O., Sanghera, G.S., Eady, R.R. and Thorneley, R.N.F. (1988). The direct electrochemistry of flavodoxin from *Azotobacter chroococcum* at a graphite electrode promoted by aminoglycosides. *Biochem. Soc. Trans. 16*, 959-960

Berggren, G., Duraffourg, N., Sahlin, M. and Sjöberg, B.M. (2014). Semiquinone-induced maturation of *Bacillus anthracis* ribonucleotide reductase by a superoxide intermediate. *J Biol Chem. 289,* 31940-31949.

Bottin, H. and Lagoutte, B. (1992). Ferredoxin and flavodoxin from the cyanobacterium *Synechocystis* sp PCC 6803. *Biochim Biophys Acta*. *1101*, 48-56.

Calderon-Gomez, L.I., Day, C.J., Hartley-Tassell, L.E., Wilson, J.C., Mendz, G.L and Korolik, V. (2017). Identification of NuoX and NuoY Ligand Binding Specificity in the *Campylobacter jejuni* Complex I. *J Bacteriol Parasitol, 8*, 307.

Cameron, A. and Gaynor, E. (2014). Hygromycin B and Apramycin Antibiotic Resistance Cassettes for Use in *Campylobacter jejuni*. *PLoS ONE 9,* e95084.

Carlone, G. M. and Anet, F. A. (1983). Detection of menaquinone-6 and a novel methyl-substituted menaquinone-6 in *Campylobacter jejuni* and *Campylobacter fetus* subsp. *fetus*. *Journal of General Microbiology, 129*, 3385-3393.

Corrado, M.E., Zanetti, G. and Mayhew, S.G. (1996). The redox potentials of flavodoxin from *Desulfovibrio vulgaris* and ferredoxin-NADP+ reductase from *Spinacia oleracea* and their complexes. *Biochem Soc Trans. 24,* 28S.

Cotruvo, J.A. Jr and Stubbe, J. (2008). NrdI, a flavodoxin involved in maintenance of the diferric-tyrosyl radical cofactor in *Escherichia coli* class 1b ribonucleotide reductase. *Proc Natl Acad Sci U S A. 105,* 14383-14388.

Cox, J., and Mann, M. (2008). MaxQuant enables high peptide identification rates, individualized p.p.b.-range mass accuracies and proteome-wide protein quantification. *Nat Biotechnol 26*, 1367-1372.

Dutton, P. L., Wilson, D. F. and Lee, C. P. (1970). Oxidation-reduction potentials of cytochromes in mitochondria. *Biochemistry 9*, 5077–5082.

Gaballa, A., Newton, G.L., Antelmann, H., Parsonage, D., Upton, H., Rawat, M., Claiborne, A., Fahey, R.C. and Helmann, J.D. (2010). Biosynthesis and functions of bacillithiol, a major low-molecular-weight thiol in Bacilli. *Proc Natl Acad Sci U S A. 107*, 6482-6486.

Gibson, D. G., Young, L., Chuang, R.Y., Venter, J.C., Hutchison 3rd, C.A., and Smith, H.O. (2009). Enzymatic assembly of DNA molecules up to several hundred kilobases. *Nature Methods, 6,* 343-345.

Gudim, I., Hammerstad, M., Lofstad, M. and Hersleth, H.P. (2018) The Characterization of Different Flavodoxin Reductase-Flavodoxin (FNR-Fld) Interactions Reveals an Efficient FNR-Fld Redox Pair and Identifies a Novel FNR Subclass. *Biochemistry*, *57*, 5427-5436.

Juhnke, H. D., Hiltscher, H., Nasiri, H. R., Schwalbe, H., and Lancaster, C. R. (2009). Production, characterization and determination of the real catalytic properties of the putative 'succinate dehydrogenase' from *Wolinella succinogenes*. *Molecular Microbiology, 71*, 1088-1101.

Haldenby, S., Bronowski, C., Nelson, C., Kenny. J., Martinez-Rodriguez, C., Chaudhuri, R., Williams, N.J., Forbes, K., Strachan, N.J., Pulman, J., Winstanley, I.N., Corless, C.E., Humphrey, T.J., Bolton, F.J., O'Brien, S.J., Hall, N., Hertz-Fowler, C. and Winstanley, C. (2000) Increasing prevalence of a fluoroquinolone resistance mutation amongst *Campylobacter jejuni* isolates from four human infectious intestinal disease studies in the United Kingdom. *PLoS One, 15*, e0227535.

Heering, H.A. and Hagen, W.R. (1996). Complex electrochemistry of flavodoxin at carbon-based electrodes: results from a combination of direct electron transfer, flavin-mediated electron transfer and comproportionation. *J. Electroanal. Chem*. *404*, 249-260

Hein, S., von Irmer, J., Gallei, M., Meusinger, R., and Simon, J. (2018). Two dedicated class C radical S-adenosylmethionine methyltransferases concertedly catalyse the synthesis of 7,8-dimethylmenaquinone. *Biochimica et Biophysica Acta - Bioenergetics, 1859*, 300–308.

Heuston, S., Begley, M., Gahan, C.G.M. and Hill, C. (2012). Isoprenoid biosynthesis in bacterial pathogens. *Microbiology 158,* 1389-1401.

Hofer, A., Crona, M., Logan, D.T. and Sjöberg, B.M. (2012) DNA building blocks: keeping control of manufacture. *Crit Rev Biochem Mol Biol*. *47*, 50-63.

Hoganson, C. W. and Babcock, G. T. (1992) Protein-tyrosyl radical interactions in photosystem II studied by electron spin resonance and electron nuclear double resonance spectroscopy: comparison with ribonucleotide reductase and in vitro tyrosine. *Biochemistry 31*, 11874-11880.

Hughes, N.J., Clayton, C.L., Chalk, P.A and Kelly, D.J. (1998). *Helicobacter pylori porCDAB* and *oorDABC* genes encode distinct pyruvate:flavodoxin and 2-oxoglutarate:acceptor oxidoreductases which mediate electron transport to NADP. *Journal of Bacteriology 180*, 1119-1128.

Johansson, R., Torrents, E., Lundin, D., Sprenger, J., Sahlin, M. and Sjöberg, B.M. and Logan, D.T. (2010). High-resolution crystal structures of the flavoprotein NrdI in oxidized and reduced states - an unusual flavodoxin. Structural biology. *FEBS J. 277,* 4265-4277.

Kendall, J.J., Barrero-Tobon, A.M., Hendrixson, D.R., and Kelly, D.J. (2014). Hemerythrins in the microaerophilic bacterium *Campylobacter jejuni* help protect key iron-sulphur cluster enzymes from oxidative damage. *Environmental Microbiology, 16*, 1105-1121.

Konrad, A., Yarunova, E., Tinta, T., Piškur, J., Liberles, D.A. (2012) The global distribution and evolution of deoxyribonucleoside kinases in bacteria. *Gene*. *492*,117-120.

Lanvers, C., Vieira Pinheiro, J.P., Hempel, G., Wuerthwein, G. and Boos, J. (2002) Analytical validation of a microplate reader-based method for the therapeutic drug monitoring of L-asparaginase in human serum. *Anal Biochem*. *309*, 117-126.

Lascelles, J. and Calder, K.M. (1985) Participation of cytochromes in some oxidation-reduction systems in *Campylobacter fetus. J. Bacteriol*. *164*, 401-409.

Liu, Y.W. and Kelly, D.J. (2015) Cytochrome *c* biogenesis in *Campylobacter jejuni* requires cytochrome c_6 (CccA; Cj1153) to maintain apocytochrome cysteine thiols in a reduced state for haem attachment. *Mol Microbiol. 96*, 1298-1317.

Lofstad, M., Gudim, I., Hammerstad, M., Røhr, Å.K. and Hersleth H.P. (2016) Activation of the Class 1b Ribonucleotide Reductase by a Flavodoxin Reductase in *Bacillus cereus*. *Biochemistry*. *55*, 4998-5001.

Mayhew, S.G. and Tollin, G. (1992). General properties of flavodoxins. In *Chemistry and biochemistry of flavoenzymes*, Vol. 3 (ed. F. Müller), pp. 389–426. CRC Press, Boca Raton, FL.

Mikheyeva, I.V., Thomas, J.M., Kolar, S.L., Corvaglia, A.R., Gaïa, N., Leo, S., Francois, P., Liu, G.Y., Rawat, M. and Cheung, A.L. (2019) YpdA, a putative bacillithiol disulfide reductase, contributes to cellular redox homeostasis and virulence in *Staphylococcus aureus*. *Mol Microbiol*. *111*, 1039-1056.

Mayhew, S.G., Foust, G. P and Massey, V. (1969) Oxidation-reduction potentials of flavodoxin from *Peptostreptococcus elsdenii*. *J. Biol. Chem*. *244*, 803-810

Parkhill, J., Wren, B. W., Mungall, K., Ketley, J. M., Churcher, C., Basham, D., Chillingworth, T., Davies, R. M., Feltwell, T., Holroyd, S., Jagels, K., Karlyshev, A. V., Moule, S., Pallen, M. J., Penn, C. W., Quail, M. A., Rajandream, M. A., Rutherford, K. M., van Vliet, A. H., Whitehead, S., & Barrell, B. G. (2000). The genome sequence of the food-borne pathogen *Campylobacter jejuni* reveals hypervariable sequences. *Nature, 403*, 665-668.

Petersson, L., Gräslund, A., Ehrenberg, A., Sjöberg, B.M and Reichard, P. (1980) The iron center in ribonucleotide reductase from *Escherichia coli*. *J Biol Chem*. *255*, 6706-6712.

Puan, K.J., Wang, H., Dairi, T., Kuzuyama, T. and Morita, C.T. (2005). *fldA* is an essential gene required in the 2-C-methyl-D-erythritol 4-phosphate pathway for isoprenoid biosynthesis. *FEBS Lett. 579*, 3802-3806.

Roca, I., Torrents, E., Sahlin, M., Gibert, I. and Sjöberg, B.M. (2008) NrdI essentiality for class 1b ribonucleotide reduction in *Streptococcus pyogenes*. *J Bacteriol*. *190*, 4849-4858.

Rohdich, F., Zepeck, F., Adam, P., Hecht, S., Kaiser, J., Laupitz, R., Gräwert, T., Amslinger, S., Eisenreich, W., Bacher, A. and Arigoni, D. (2003). The deoxyxylulose phosphate pathway of isoprenoid biosynthesis: studies on the mechanisms of the reactions catalyzed by IspG and IspH protein. *Proc Natl Acad Sci U S A. 100,* 1586-1591.

Rusling J. F. (1998) Enzyme Bioelectrochemistry in Cast Biomembrane-Like Films. *Accounts of Chemical Research 31*, 363-369.

Sahlin, M., Petersson, L., Gräslund, A., Ehrenberg, A., Sjöberg, B. M. and Thelander, L. (1987) Magnetic interaction between the tyrosyl free radical and the antiferromagnetically coupled iron center in ribonucleotide reductase. *Biochemistry 26*, 5541-5548.

Salillas, S. and Sancho, J. (2020) Flavodoxins as Novel Therapeutic Targets against *Helicobacter pylori* and Other Gastric Pathogens. *Int J Mol Sci. 21*, 1881.

Sancho, J. (2006) Flavodoxins: sequence, folding, binding, function and beyond. *Cell Mol Life Sci*. *63,* 855-864.

Sandrini, M.P., Clausen, A.R., Munch-Petersen, B. and Piskur, J. (2006) Thymidine kinase diversity in bacteria. *Nucleosides Nucleotides Nucleic Acids*. *25*, 1153-1158.

Seagel, H.M., Spatzal, T., Hill, M.G., Udit, A.K. and Rees, D.C. (2017) Electrochemical and structural characterization of *Azotobacter vinelandii* flavodoxin II. *Protein Science 26*, 1984-1993.

Sellars, M.J., Hall, S.J., and Kelly, D.J. (2002). Growth of *Campylobacter jejuni* supported by respiration of fumarate, nitrate, nitrite, trimethylamine-N-oxide, or dimethyl sulfoxide requires oxygen. *Journal of Bacteriology, 184*, 4187-4196.

Sheppard, S. K., Dallas, J. F., Strachan, N. J. C., MacRae, M., McCarthy, N. D., Wilson, D. J., Gormley, F. J., Falush, D., Ogden, I. D., Maiden, M. C., and Forbes, K. J. (2009). *Campylobacter* genotyping to determine the source of human infection. *Clinical Infectious Diseases, 8,* 1072–1078.

Smith, M.A., Finel, M., Korolik, V. and Mendz, G.L. (2000) Characteristics of the aerobic respiratory chains of the microaerophiles *Campylobacter jejuni* and *Helicobacter pylori*. *Arch Microbiol 174*, 1-10.

St Maurice, M., Cremades, N., Croxen, M.A., Sisson, G., Sancho, J. and Hoffman, P.S. (2007). Flavodoxin:quinone reductase (FqrB): a redox partner of pyruvate:ferredoxin oxidoreductase that reversibly couples pyruvate oxidation to NADPH production in *Helicobacter pylori* and *Campylobacter jejuni. J Bacteriol. 189,* 4764-4773.

Stubbe. J. and Cotruvo. J.A. Jr. (2011) Control of metallation and active cofactor assembly in the class 1a and 1b ribonucleotide reductases: diiron or dimanganese? *Curr Opin Chem Biol 15*, 284-90.

Taylor, A.J. and Kelly, D.J. (2019) The function, biogenesis and regulation of the electron transport chains in *Campylobacter jejuni*: New insights into the bioenergetics of a major food-borne pathogen. *Adv Microb Physiol 74*, 239-329.

Torrents, E. (2014) Ribonucleotide reductases: essential enzymes for bacterial life. *Front Cell Infect Microbiol*. 4, 52.

van der Stel, A. X., Boogerd, F. C., Huynh, S., Parker, C. T., van Dijk, L., van Putten, J. P. M., and Wösten M. M. S. M. (2017). Generation of the membrane potential and its impact on the motility, ATP production and growth in *Campylobacter jejuni*. *Molecular Microbiology, 105*, 637-651.

Yahara, K., Méric, G., Taylor, A. J., de Vries, S. P. W., Murray, S., Pascoe, B., Mageiros, L., Torralbo, A., Vidal, A., Ridley, A., Komukai, S., Wimalarathna, H., Cody, A. J., Colles, F. M., McCarthy, N., Harris, D., Bray J. E., Jolley, K. A., Maiden, M. C., Bentley, S. D., Parkhill, J., Bayliss, C. D., Grant, A., Maskell, D., Didelot, X., Kelly, D. J., and Sheppard, S. K. (2017). Genome-wide association of functional traits linked with *Campylobacter jejuni* survival from farm to fork. *Environmental Microbiology, 19*, 361–380.

van Vliet, A.H., Wooldridge, K.G. and Ketley, J.M. Iron-responsive gene regulation in a *Campylobacter jejuni fur* mutant. *J Bacteriol*. 180, 5291-5298.

Wang, M., Feng, W.Y., Zhao, Y.L. and Chai, Z.F. (2010) ICP-MS-based strategies for protein quantification. *Mass Spectrom Rev, 29*, 326-438.

Weerakoon, D.R. and Olson, J.W. (2008). The *Campylobacter jejuni* NADH:ubiquinone oxidoreductase (complex I) utilizes flavodoxin rather than NADH. *Journal of Bacteriology 190,* 915-925.

Wu, C.H, Jiang, W., Krebs, C. and Stubbe, J. (2007) YfaE, a ferredoxin involved in diferric-tyrosyl radical maintenance in *Escherichia coli* ribonucleotide reductase. *Biochemistry. 46*, 11577-11588.

Table 1. Comparison of redox potentials and FMN binding loop regions in selected flavodoxins and NrdI proteins

Species	Protein	pI	E_1 (mV)	E_2 (mV)	Δ (mV)	50s (W) loop	90s (Y) loop	Ref
D. vulgaris	Fld	4.0	- 440	- 143	297	STWGDDSIE	DSS--YE	[1]
Synechocystis	Fld	3.5	- 433	- 238	195	PTWWVGELQ	DQVGYAD	[2]
A. vinlandii	Fld	4.4	- 483	- 187	296	PTLGEGELP	DQVGYPE	[3]
C. jejuni	Fld	3.9	- 190	- 170	20	STWGSGDLQ	DSESYSD	This study
						40s loop	**70s loop**	
E. coli	NrdI	9.4	- 255	- 264	-9	GGGGTAG	NRNFGEA	[4]
B. cereus	NrdI	5.0	- 309	- 252	57	GFGNVPER	NRNWGDM	[5]
B. anthracis	NrdI	5.4	- 385	- 270	115	GFGNVPER	NRNWGDM	[6]

The FMN is sandwiched between two loop regions known as the 50s or W-loop and 90s or Y-loop in classical flavodoxins, or the 40s loop and 70s loop in NrdI proteins. These contain aromatic/hydrophobic residues (highlighted in orange) that stack over the isoalloxazine ring. A preponderance of anionic residues (blue) in the loops in flavodoxins is thought to contribute to lowering of the E_1 redox potential in particular, while in NrdI proteins the environment is more neutral or charge compensated (cationic residues in red). References: [1], Corrado et al. (1996);

[2], Bottin and Langoutte (1992); [3], Segal et al. (2017); [4] Cotruvo and Stubbe (2008); [5], Gudim et al. (2018); [6], Berggren et al. (2014).

Table 2. Primers used in this work. Underlined bases are adaptor regions corresponding to the pGEM3zf vector (ISA F and R primers) or to the kanamycin resistance cassette (ISA KR and KF primers). COMP primers were used for complementation in the pRRA vector (MfeI site in bold; XbaI site in italics) and OE primers for overexpression in pET21a (NdeI sites underlined in bold; XhoI sites underlined in italics).

	Primer sequence 5′-3′
FQRB_ISA_F1F	GAGCTCGGTACCCGGGGATCCTCTAGAGTCCATTTGTAAATTTTG CTTCA
FQRB_ISA_F1KR	AAGCTGTCAAACATGAGAACCAAGGAGAATGACCTGCACCTACT ACAATT
FQRB_ISA_F2KF	GAATTGTTTTAGTACCTAGCCAAGGTGTGCAGCAAGTATAGTTAC AGGGTTA
FQRB_ISA_F2R	AGAATACTCAAGCTTGCATGCCTGCAGGTCAATACTCCAAAATTC CGAT
FQRB_COMP_F	ACAC**CAATTG**CATCTAACAAAAGCCTATCTTT
FQRB_COMP_R	ACAC*TCTAGA*TTATTTTGCATATGAATTTTCTAG
FLDA_OE_F	TATATT**CATATG**TCAGTAGCAGTAATCTATGGTAGT
FLDA_OE_R	ATTTAT*CTCGAG*AGCAAAATAAGGTTTGATTT
FQRB_OE_F	TATATT**CATATG**AAAAAAATAGATTTAATTGTAGTAGG
FQRB_OE_R	ATTTAT*CTCGAG*AAGCACAGAAAGAATTTTCA
NRDB_OE_F	TATATT**CATATG**CAAAGAAAAAGAATTTACAATC
NRDB_OE_R	ATTTAT*CTCGAG***GAAGTCATCAAAGCTTATACTACC**
KAN_F	ATTCTCCTTGGTTCTCATGTTTGACAGCTTAT
KAN_R	GCACACCTTGGCTAGGTACTAAAACAATTC

Figure legends

Figure 1. Redox properties of the *C. jejuni* flavodoxin FldA. In (**A**) the electronic absorption spectra of the fully oxidized (orange), semi-reduced (purple) and fully reduced (blue) states of FldA are shown. The spectra were recorded for 50 μM protein in an anaerobic buffer (50 mM potassium phosphate buffer, pH 7.0. Path length = 1 cm). The semi-reduced state was produced by stoichiometric addition of sodium dithionite. Excess dithionite was added to obtain the fully-reduced state. (**B**) optically monitored potentiometric titration of FldA at 610 nm. The data (blue circles) and fit (dashed line) to the equation describing sequential one electron additions to a centre with E_2 = -170 mV and E_1 = -190 mV. Sample contained 50 μM protein in an anaerobic buffer (10 mM potassium phosphate buffer, pH 7.0.) Path length = 1 cm. (**C**) Cyclic voltammetry of CjFldA (continuous blue line) adsorbed on a DDAB-coated pyrolytic graphite edge electrode. Cyclic voltammetry of the DDAB-coated electrode alone is also shown (broken grey line). Measurements performed in 50 mM potassium phosphate, pH 7 at 20 °C with a scan rate of 20 mV s^{-1}. (**D**) Reduction of CjFldA by electrons from pyruvate via POR (red trace) or 2-oxoglutarate via OOR (Blue trace) in cell-free extracts monitored at 460 nm, as described in Experimental Procedures. The traces are an average of two determinations (raw data in supplementary file).

Figure 2. FqrB is related to flavodoxin reductases in Gram-positive bacteria and is an NADPH specific FldA reductase. (**A**) Phylogenetic tree of a selection of PNDOR enzymes from Gram-negative and Gram-positive bacteria. A multiple sequence alignment was generated in CLUSTAL omega then JALVIEW used to construct the tree shown. Sequences were obtained from UNIPROT. Genus abbreviations; *A., Arcobacter; B., Bacillus; Bo., Borrelia; C. Campylobacter; E., Escherichia; H., Helicobacter; L., Lactobacillus; S., Staphylococcus; St., Streptococcus*. (**B**) UV-VIS absorption spectrum of purifed *C. jejuni* FqrB (50 μM) with FAD peaks at 375 nm and 460 nm. (**C**) NADPH dependent reduction of FldA catalysed by FqrB. The

absorbance spectrum of a mixture of FldA (50 μM) and FqrB (0.1 μM) in 50 mM Tris-HCl buffer pH 7.5 was recorded alone (red trace) or 5 min after the addition of NADPH (0.15 mM final concentration). The *inset* shows a kinetic trace at 460 nm, to show the FldA FMN reduction. (**D**) same as (**C**) but with NADH.

Figure 3. Growth phenotypes of wild-type, *fqrB* mutant and complemented strains and effect of deoxyribonucleosides or toxic analogues. In (**A**) growth curves of wild-type (left panel), *fqrB* mutant (middle panel) and complemented strain (right panel) under standard microaerobic conditions in complex MHS media are shown in the absence or the presence of the indicated concentrations of a mixture of the 4 deoxyribonucleosides (dRNS). The data points are means of triplicate independent cultures with error bars indicating SD. For the *fqrB* mutant, Student's t-test was used to examine the signficance of the effect of 0.1 mM dRNS compared to control (**** P<0.0001; ** *P* <0.01; * *P* <0.05). In (**B**) the effect of the toxic nucleotide analogues 6-thioguanine (TG) and 6-mercaptopurine (MP) on wild-type (black bars), *fqrB* mutant (red bars) and complemented strain (blue bars) were evaluated by growth in MHS media. Cultures as in (A) were set up in triplicate and the OD600 nm measured after 12 h. The data are expressed as a ratio of the controls without TG or MP addition. Error bars show SD and the significance of the effect of TG or MP estimated by Student's t-test (** *P* <0.01; * *P* <0.05).

Figure 4. Characterisation of the NrdB subunit of *C. jejuni* RNR. His-tagged NrdB was purified from *E. coli* BL21 (pETNrdB) as described in Experimental Procedures. **(A)** Iron (orange) and manganese (pink) content of NrdB, measured by ICP-MS. The data are the means and SD of 3 independent purifications from cells grown in LB alone, LB + Fe (50 μM ferrous ammonium sulphate) or LB + Mn (50 μM manganese chloride). The sulfur content of the samples was used to normalize the data to the protein content (Wang et al., 2010) and is expressed as a molar ratio. In each case the Mn ratio is significantly lower than the Fe ratio (****, *P* <0.0001 by Students t-test). (**B**) Optical absorption spectroscopy of NrdB. The blue trace shows the spectrum of as-purifed NrdB (100 μM) with the tyrosyl radical peak at 411 nm and charge transfer bands of the di-ferric centre at 325 nm and 370 nm. The red trace shows the spectrum after 30 min treatment with 1 mM hydroxylamine (HA), which quenches the radical. The black trace is the difference spectrum, illustrating the tyrosyl radical contribution. The EPR spectrum in (**C**) shows that HA treatment does not significantly alter the g = 4.27 CW EPR signal of the high spin ferric iron in rhombic coordination in 50 ⌈M NrdB as isolated (blue trace) or 50 ⌈M NrdB + 1 mM hydroxylamine (red trace). Instrumental conditions used were: microwave frequency ⌇ $_{MW}$ = 9.47 GHz; microwave power P_{MW} = 3.165 mW; sweep rate v = 22.65 G/s (one scan); time constant ⏐ =

81.92 ms; modulation amplitude A_m = 5 G; modulation frequency ν_m = 100 kHz; registration temperature T = 10 K. In (**D**), optical spectroscopy (50 μM NrdB) shows that a high concentration of hydroxyurea (HU), either with (blue trace) or without (red trace) EDTA does not appreciably quench the tyrosyl radical compared to HA in panel (B).

Figure 5. Reduced flavodoxin catalyses tyrosyl radical regeneration in NrdB. In (A) a mixture of hydroxylamine-treated NrdB (50 μM final concentration), FldA (50 μM), FqrB (5 μM) and NADPH (1 mM) in 50 mM Tris-HCl buffer pH 7.5 was incubated at 37 °C and spectra recorded at the times shown. The build-up of the tyrosyl radical in NrdB is evident at 411 nm. In (B) the spectra of a series of control incubations missing one of the components in (A), as indicated, was obtained after 80 min incubation at 37 °C. In (C) the same mixture as in panel (A) was prepared, incubated for 80 min and the optical spectra compared with as-purifed NrdB and HA-treated NrdB. These same samples were then examined by EPR spectroscopy (D) as described in Experimental Procedures. The free radical area of the CW EPR spectra of NrdB is shown: 50 μM NrdB as isolated shows a typical EPR line shape of a RNR tyrosyl radical (black trace); 50 μM NrdB +1 mM hydroxylamine results in essentially complete reduction of the radicals (red trace); the free radical reconstituted by 50 μM flavodoxin (FldA) and 5 μM flavodoxin reductase (FqrB) in the presence of 1 mM NADPH (blue trace) has a line shape indistinguishable from that of NrdB as isolated. The instrumental conditions were: microwave frequency ν_{MW} = 9.47091 GHz (blue trace), 9.46769 GHz (black trace) and 9.47058 GHz (red trace; the three spectra were shifted along the magnetic field axis to a common g-value on the basis of these differences in the microwave frequencies); P_{MW} = 5.016 x 10^{-2} mW; v = 0.596 G/s (one scan); τ = 81.92 ms; A_m = 3 G; ν_m = 100 kHz; T = 10 K. Symbol "x" gives relative magnification of the spectra.

Figure 6. Superoxide can catalyse tyrosyl radical formation in NrdB *in vitro*. In (A), the complete reconstituted system of HA-treated NrdB (50 μM), FldA (50 μM), FqrB (5 μM) and NADPH (1 mM) was incubated at 37 °C for 120 min as a control to show formation of the tyrosyl radical at 411 nm. In (B) the same components were incubated but with the addition of 20 units of SOD and the spectra recorded at 20 min intervals for the times shown. In (C), HA-treated NrdB

alone (50 μM) was incubated at 37 °C with 1 mM hypoxanthine and 0.5 units of xanthine oxidase for 3 h and spectra recorded every 30 min as shown.

Figure 7. Multiple pathways for FldA reduction and the role of FldA in electron transport, isoprenoid biosynthesis and deoxyribonucleotide reduction. FldA can be reduced by electrons from at least three sources; from pyruvate oxidation via pyruvate:flavodoxin oxidoreductase (POR), from 2-oxoglutarate reduction via 2-oxoglutarate:flavodoxin oxidoreductase (OOR) or from NADPH oxidation via flavodoxin quinone reductase (FqrB). FldA is the only known electron donor for respiratory Complex I in *C. jejuni* but given the relatively small redox potential difference (~ 100 mV) between $FldA_{ox}/FldA_{red}$ couple and the menaquinone (MK)/menaquinol (MKH_2) couple it is unclear if Complex I is proton translocating. Our results suggest that FldA is an electron donor to the NrdB subunit of ribonucleotide reductase (RNR), to generate the tyrosine radical (Y•). This is then transferred to the NrdA subunit to generate a radical at the active site cysteine (C•), necessary for reduction of ribonucleotides (RNTs) to deoxyribonucleotides (dRNTs). FldA is also thought to be required as a source of electrons for two consecutive steps in the final section of the MEP isoprenoid biosynthesis pathway, catalysed by IspG which converts methylerythritol cyclic pyrophosphate (MEc-PP) into 4-hydroxy-3-methylbut-2-enyl pyrophosphate (HMB-PP) and IspH which converts HMB-PP into the products isopentyl pyrophosphate (IPP) and dimethylallyl pyrophosphate (DMAPP). MEc-PP is produced in several enzymatic steps from pyruvate and glyceraldehyde-3-phosphate (GA3P).

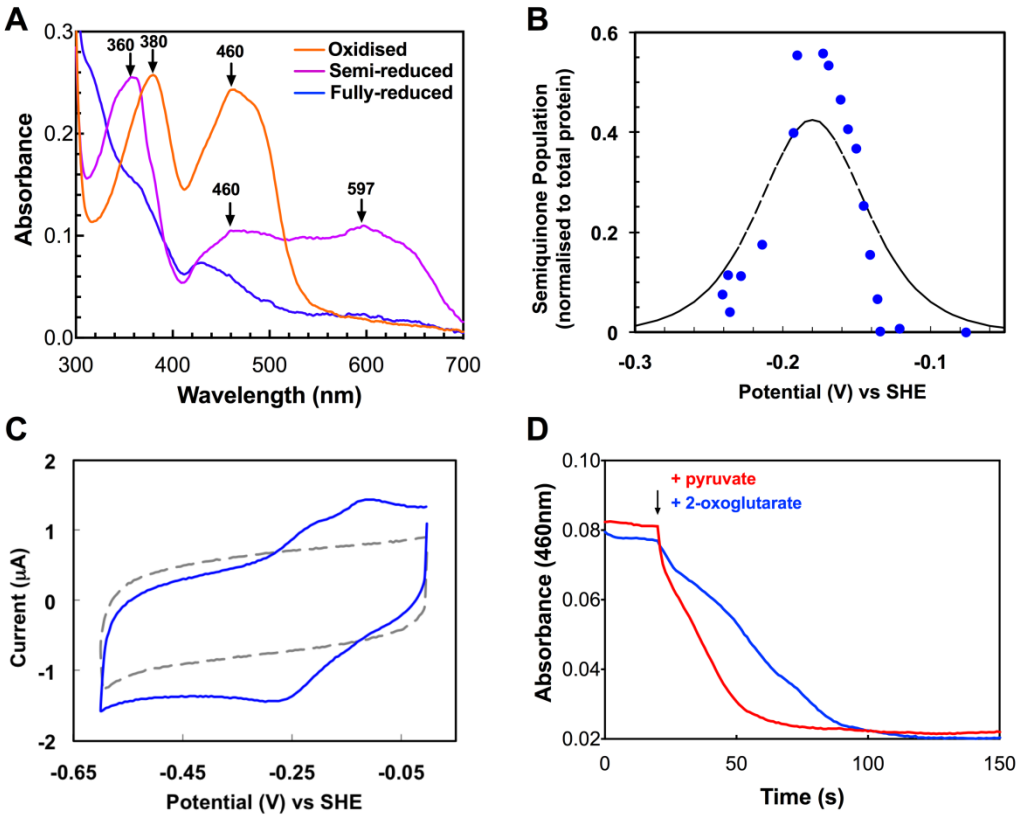

mmi_14715_f1.tiff

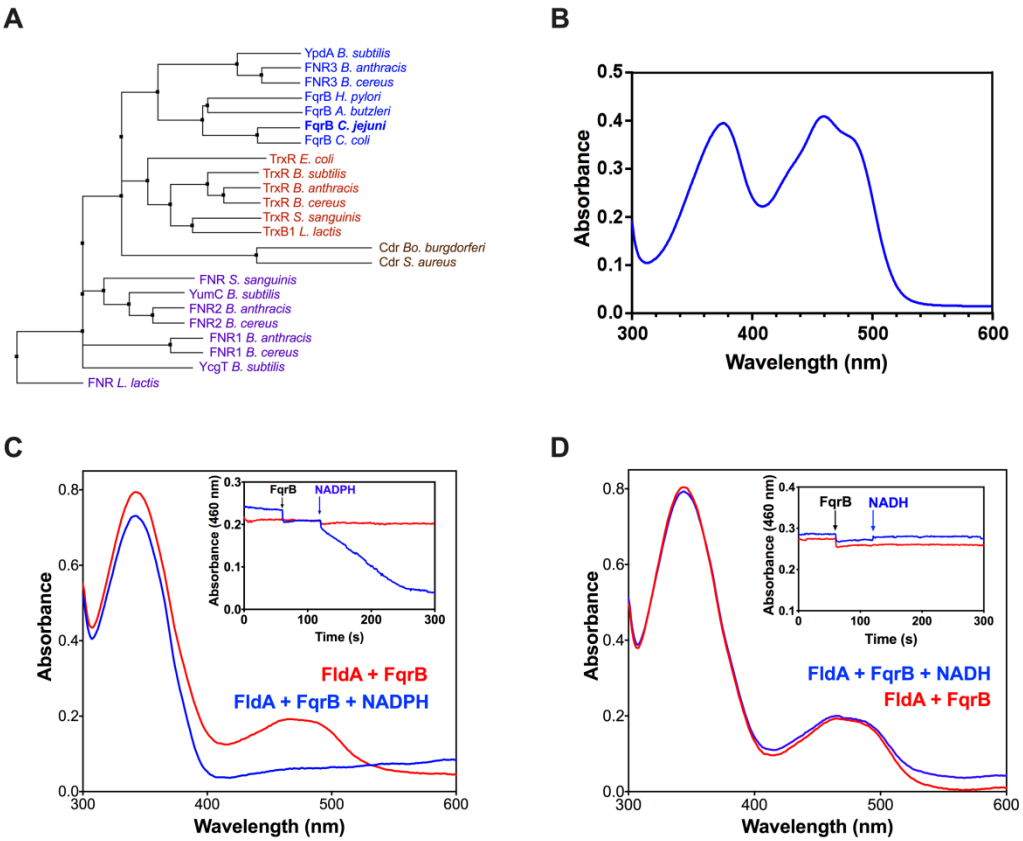

mmi_14715_f2.tiff

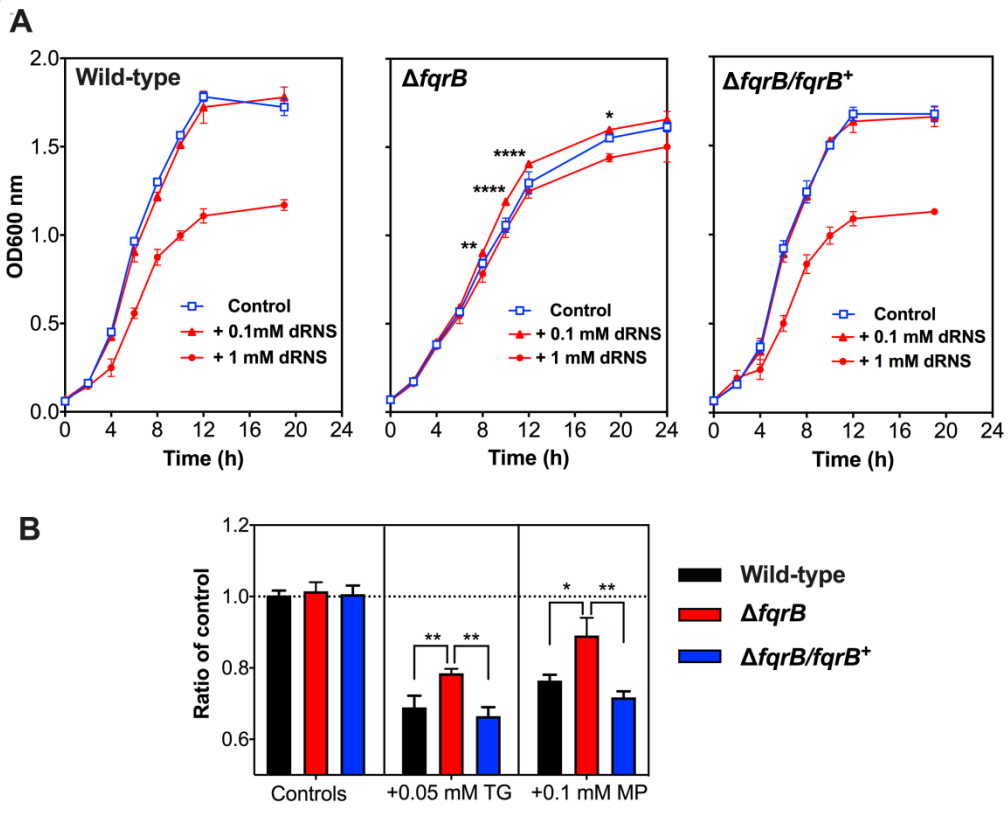

mmi_14715_f3.tiff

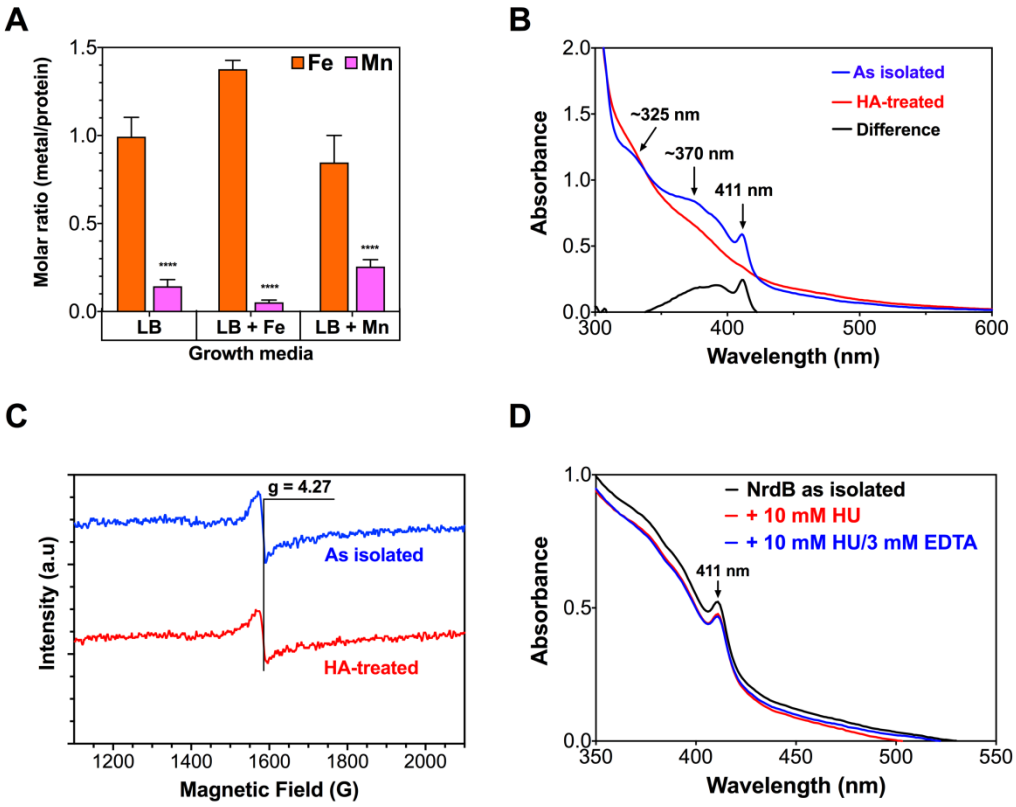

mmi_14715_f4.tiff

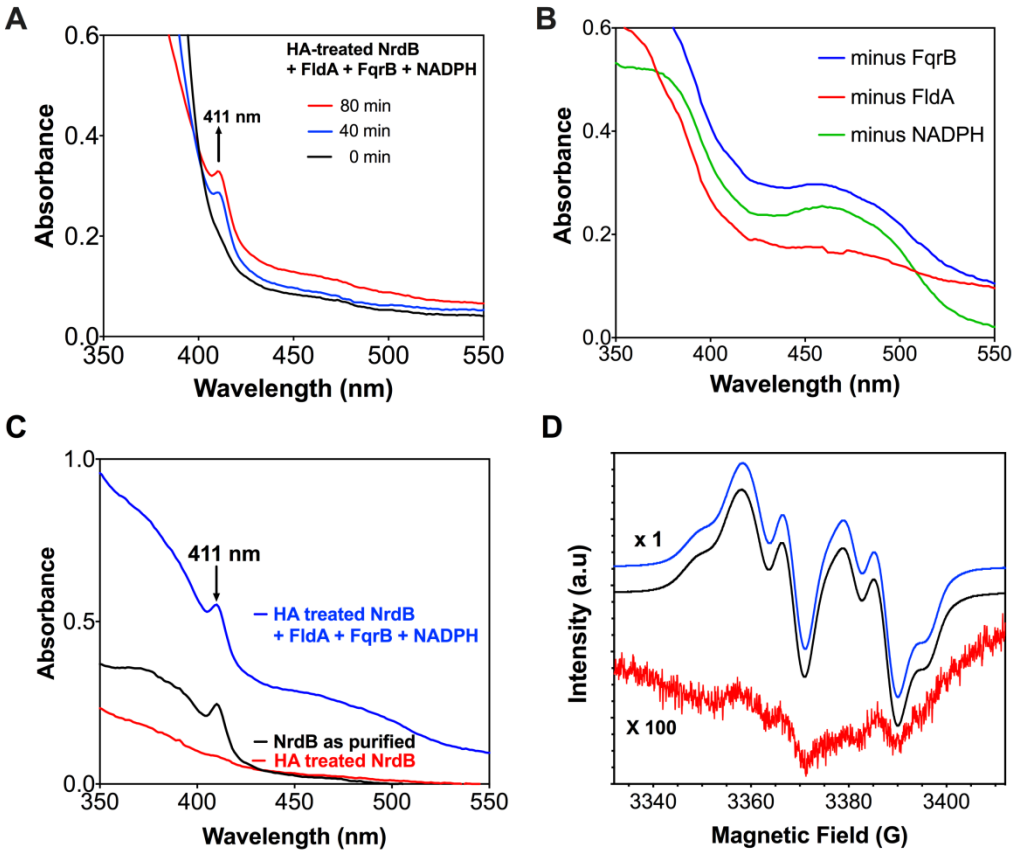

mmi_14715_f5.tiff

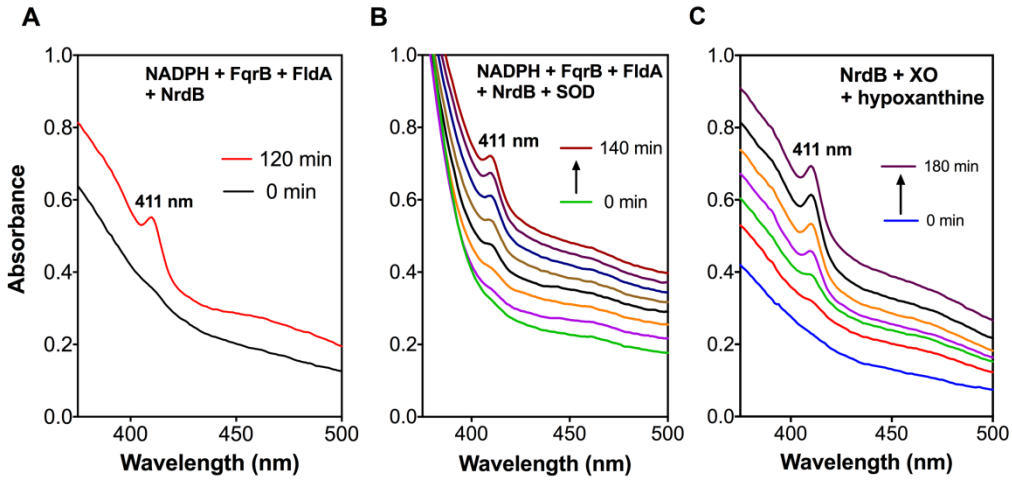

mmi_14715_f6.tiff

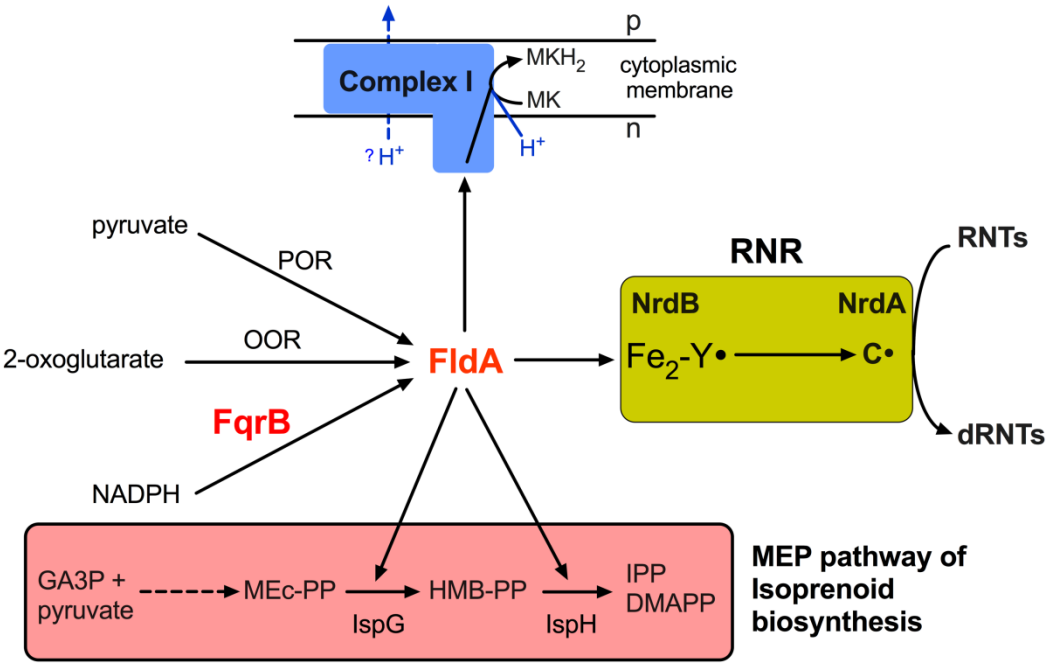

mmi_14715_f7.tiff